

# $\alpha$ -sarcin and RNase T1 based immunoconjugates: the role of intracellular trafficking in cytotoxic efficiency

Jaime Tomé-Amat<sup>1,2</sup>, Javier Ruiz-de-la-Herrán<sup>1</sup>, Álvaro Martínez-del-Pozo<sup>1</sup>, José G. Gavilanes<sup>1</sup> and Javier Lacadena<sup>1</sup>

<sup>1</sup> Departamento de Bioquímica y Biología Molecular I, Universidad Complutense de Madrid, Spain

<sup>2</sup> Department of Food Science, Cornell University, Ithaca, NY, USA

## Keywords

colon cancer; immunotoxin; RNase T1; trafficking;  $\alpha$ -sarcin

## Correspondence

J. Lacadena, Departamento de Bioquímica y Biología Molecular I, Facultad de Ciencias Químicas, Universidad Complutense, 28040 Madrid, Spain  
Fax: +34913944159  
Tel: +34913944259  
E-mail: jlacaden@quim.ucm.es

(Received 23 June 2014, revised 7 November 2014, accepted 2 December 2014)

doi:10.1111/febs.13169

Toxins have been thoroughly studied for their use as therapeutic agents in search of an improvement in toxic efficiency together with a minimization of their undesired side effects. Different studies have shown how toxins can follow different intracellular pathways which are connected with their cytotoxic action inside the cells. The work herein presented describes the different pathways followed by the ribotoxin  $\alpha$ -sarcin and the fungal RNase T1, as toxic domains of immunoconjugates with identical binding domain, the single chain variable fragment of a monoclonal antibody raised against the glycoprotein A33. According to the results obtained both immunoconjugates enter the cells via early endosomes and, while  $\alpha$ -sarcin can translocate directly into the cytosol to exert its deathly action, RNase T1 follows a pathway that involves lysosomes and the Golgi apparatus. These facts contribute to explaining the different cytotoxicity observed against their targeted cells, and reveal how the innate properties of the toxic domain, apart from its catalytic features, can be a key factor to be considered for immunotoxin optimization.

## Introduction

Immunotoxins embody the idea proposed by Paul Ehrlich when he defined as magic bullets agents with the ability to specifically target just one kind of cells and therefore exert a highly specific therapeutic action without any unwanted side effects [1]. They are chimeric proteins composed of two domains: the target domain, usually a whole antibody or a fragment which specifically targets a tumor marker, and the toxic domain, responsible for the cytotoxicity [2,3]. Three major types of toxins are used as toxic domains, depending on their mode of action [4]. Type I consists of enzymes that interact with the lipidic component of the membranes and, once inside the cells, modify intracellular functions causing cell death. Type II refers to toxins that, after binding to a cellular receptor, are

internalized and then kill the cells. Type III involves those toxins capable of forming pores in the cellular membrane, leading to cell death. Thus, many different toxins have been used to construct immunotoxins, e.g. ricin chain A [5], nigrin b [6], gelonin [7], saporin [8], *Diphtheria* toxin [9], *Pseudomonas* toxin [10], anthrax toxin [11], barnase [12] or  $\alpha$ -sarcin [13], which behave as type I toxins. On the other hand, tumor necrosis factor [14] and sTRAIL [15] are type II toxins, while actinoporins [16,17], cyt A endotoxin [18] and cecropin belong to the group of type III toxins.

The *in vitro* toxicity of an immunotoxin depends on several molecular aspects, including antigen binding affinity, internalization rate, intracellular processing, toxin release and intrinsic toxicity [19]. Intracellular

## Abbreviations

DAPI, 4',6-diamidino-2-phenylindole; GAR, goat anti-rabbit; GPA33, glycoprotein A33; IMTXA33 $\alpha$ S, immunotoxin based on the fusion of scFvA33 and  $\alpha$ -sarcin; MTT, 3-(4,5-dimethylthiazol-2-yl)-2,5-diphenyl-tetrazolium bromide; scFvA33T1, immunoRNase based on the fusion of scFv A33 and RNase T1; scFv, single chain variable fragment.

trafficking of the toxin appears to be a checkpoint for the desired cytotoxic effects [20]. Once they have entered cells, protein toxins are found in early endosomes that can be later recycled or degraded in the lysosomes. Subsequent intracellular trafficking, release and endosomal escape are often achieved using intrinsic toxin features. Two main pathways are usually followed, direct translocation to the cytosol or the retrograde route via the Golgi apparatus. Thus, the ability to deliver the toxin to the cytosol is commonly considered to be the rate-limiting step in cytotoxic efficiency [7].

Clinical trials using immunotoxins have led to studies regarding their optimization focused on both target and toxic domains, although the target domain is the one which has evolved more over the years [3,21,22]. Thus, immunotoxins were initially designed containing the entire antibody which soon was replaced by the Fab domain, the single chain variable fragment (scFv) or even solely two antibody complementary determinant regions, aiming to achieve size optimization [3,23–25]. Along with these studies, others have focused on the stability of the construct [26], the use of different adjuvants [27–29] or modifications to improve specificity by combining two or more different binding domains to obtain diabodies or triabodies [30–32].

Within the last decade, new proteins have also emerged to be used as toxic domains. Using this idea, RNases from different sources have become a very popular choice, giving rise to what has been called the group of immunoRNases [33–35]. The use of proenzymes which only become toxic once they are activated inside the cell [36] is another promising approach. However, few studies have focused on increasing the efficiency of the toxic domain [37] or modulating its intracellular trafficking [38].

The immunoconjugates studied here use as binding domain the scFv portion of a monoclonal antibody (scFvA33) which targets the tumor specific antigen GPA33, a membrane glycoprotein overexpressed in 95% of colon cancer cells and absent in other types of tumor or healthy tissues [39]. The role of this antigen is still unknown, although it is thought to be involved in keeping the mucosal integrity of the small intestine during embryonic development [40]. In addition, the intracellular pathway of the internalized antigen remains unknown except for the fact that it could happen via macropinosomes [41]. This binding domain was combined to two different, but structurally related, RNases as toxic domains. In the first design, scFvA33 was linked to the fungal ribotoxin  $\alpha$ -sarcin [42] giving as a result the IMTXA33 $\alpha$ S immunotoxin

[13]. The second immunoRNase linked the same binding domain to fungal RNase T1 [43], resulting in the scFvA33T1 construct [44]. Both immunoRNases have been characterized in great detail from the structural and functional points of view [13,44] and thus represent excellent models to study the effect of intracellular trafficking on immunotoxin cytotoxicity. Accordingly, the work presented now focuses on the different pathways followed by the two toxic domains and demonstrates how they determine the different cytotoxic effectiveness observed between them.

## Results

### Immunotoxin and immunoRNase labeling

In order to study the binding and routes followed by the two constructs, the chimeric proteins were labeled with Alexa 555. The immunoRNase was labeled at pH 8.0, but the immunotoxin was labeled at pH 7.0 given

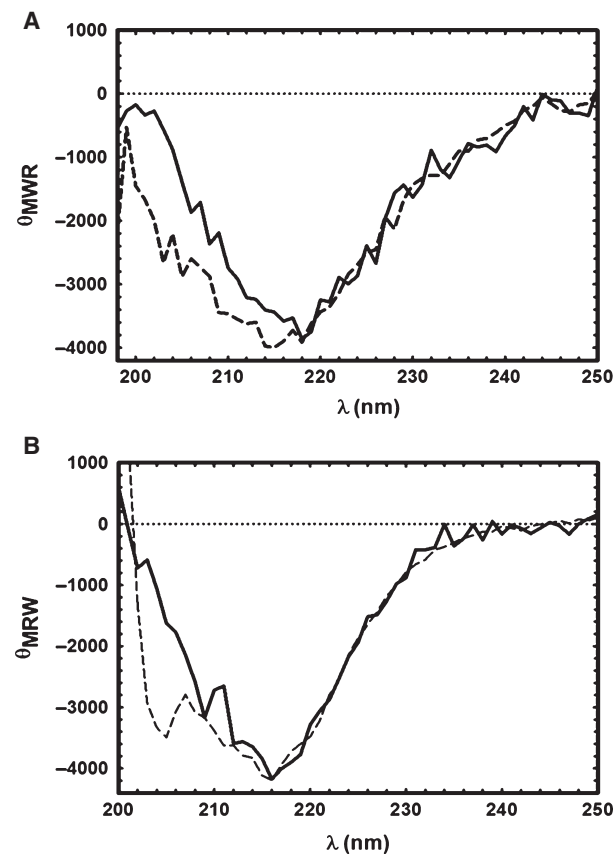


**Fig. 1.** Far-UV CD spectra of (A) IMTXA33 $\alpha$ S and (B) scFvA33T1. In both cases the solid line corresponds to the unlabeled protein, while the spectra of the proteins labeled with Alexa 555 appear as dashed lines.

that  $\alpha$ -sarcin is partially denatured around that pH value [45] and assuming that the lower degree of labeling would be compensated by the presence of 17 amine groups more than the immunoRNase, as RNase T1 is an acidic protein [43]. Once both constructs were labeled, far-UV CD spectra were registered in order to compare the conformations of both the unlabeled and labeled molecules. As can be seen in Fig. 1, both modified proteins remain fully structured as the unlabeled versions.

### Internalization studies

Binding of the two immunoconjugates to SW1222 cells has been reported previously [13,44]. Thus, internalization of both labeled constructs was studied after incubation for 16 h. The images obtained (Fig. 2) showed how both chimeric proteins, immunotoxin and immunoRNase, were internalized into the target cells. In addition, and only in the case of IMTXA33 $\alpha$ S, the immunoconjugate sometimes appeared within large sized vesicles (data not shown), previously described as macropinosomes [41].

### Endosome colocalization

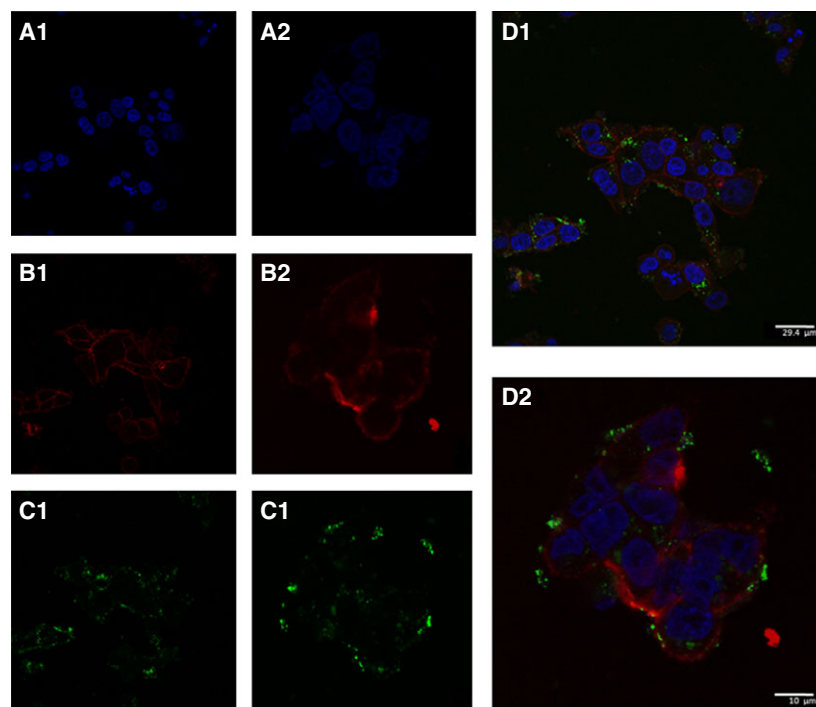
To describe the intracellular pathway in more detail, colocalization with endosomes was also studied. With this purpose, endosomes were labeled using an

antibody targeting the protein A1, present in early endosomes [46]. As shown in Fig. 3, the results indicated partial colocalization of both immunoconjugates with early endosomes. Quantitative colocalization analysis showed values between 10% and 30% of colocalization. Arrows on the figure show some examples where colocalization with endosomes was found. In this case, no significant differences were found between the two immunoconjugates.

### Lysosomes–Golgi colocalization

As described above, two main pathways are usually followed by toxins once they are localized in endosomes: via lysosomes or via the Golgi apparatus. To distinguish between the two organelles, different markers were used as described in Materials and methods: LysoTracker, a fluorescent acidotropic probe specific to lysosomes [47], and wheat germ agglutinin, which recognizes the highly abundant sialic acid of Golgi membranes [48]. The images obtained for lysosomes are shown in Figs 4 and 5. Partial colocalization was found between the immunoRNase and lysosomes. Quantitative analysis of the degree of colocalization, at the two times assayed, showed values around 50% of colocalization. This degree of colocalization was dramatically decreased when the antibiotic bafilomycin, which inhibits lysosomal acidification, was added (Fig. 4). However, no colocalization was observed with

**Fig. 2.** Immunofluorescence microscopy images of SW1222 cells incubated with IMTXA33 $\alpha$ S-555 (1) or scFvA33T1-555 (2), 25  $\mu\text{g}\cdot\text{mL}^{-1}$ , for 16 h to analyze protein internalization. (A) DAPI staining of nuclei; (B) plasmatic membrane staining using anti-CD44 and GAM-Alexa 647; (C) fluorescence corresponding to IMTXA33 $\alpha$ S-555 or scFvA33T1-555. (D) Images corresponding to merging of the three channels.



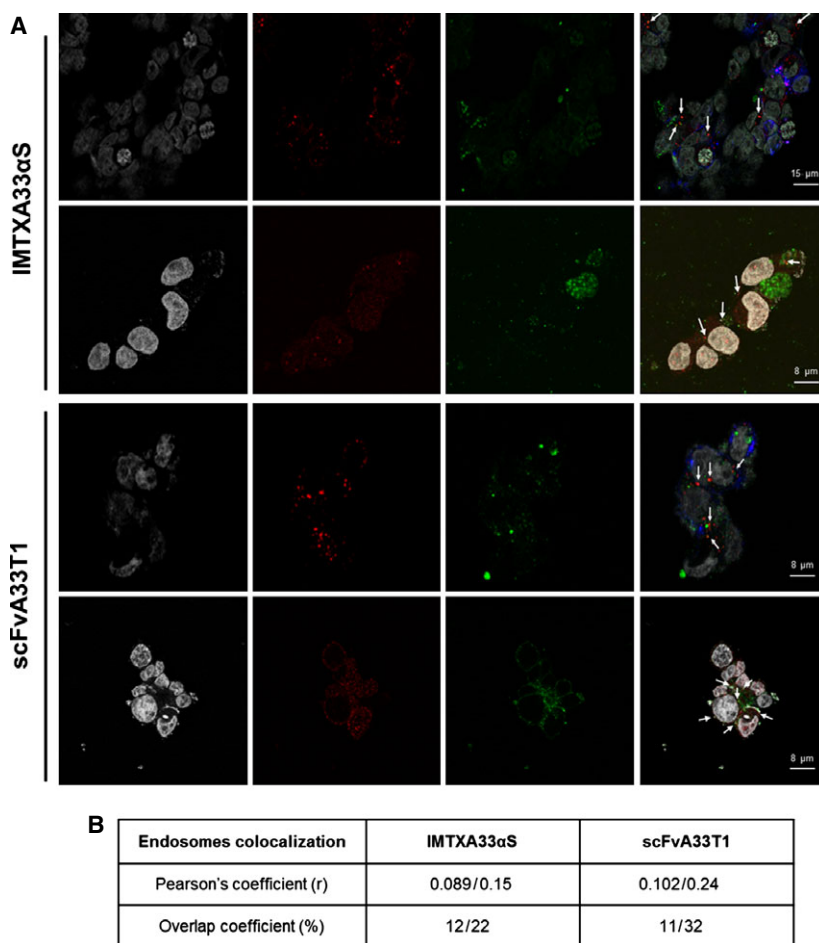


**Fig. 3.** Immunofluorescence confocal microscopy images of SW1222 cells incubated for 2 h with IMTXA33αS-555 or scFvA33T1-555 to analyze colocalization with endosomes. (A) Two sets of images for each immunoconjugate are shown. Columns (from left to right) correspond to nuclei labeled with DAPI, early endosomes labeled with anti-EEA1 and GAR-Alexa 488, IMTXA33αS-555 or scFvA33T1-555 and images corresponding to merging of the three channels. Arrows indicate some sites of colocalization. (B) Quantitative colocalization analysis as indicated in Materials and methods.

the α-sarcin based immunotoxin at the two times assayed (Fig. 5).

On the other hand, when the same experiment was developed using the Golgi-specific probe, colocalization was found for both immunotoxin and immunoRNase (Fig. 6), the fluorescence signal being more intense for the latter, with degrees of colocalization around 45% and 65%, respectively, for the longest time assayed.

### Cell viability assay

There is an inner relationship between the internal pathway followed by toxins and the lethality of the immunoconjugates. Accordingly, once the pathway followed by each construct was studied, we proceeded to analyze their toxic action. This specific cytotoxicity had been previously reported, obtaining IC<sub>50</sub> values in the nanomolar range for the α-sarcin based immunotoxin [13] and in the micromolar range for the immunoRNase [44]. These assays, however, were performed in different conditions for the

two immunoconjugates given that the two toxic domains employed have different mechanisms of action [42,43,49]. Therefore, cell viability experiments [3-(4,5-dimethylthiazol-2-yl)-2,5-diphenyl-tetrazolium bromide (MTT) or protein biosynthesis inhibition assays] were developed in identical conditions in order to compare the toxic action of the two proteins against SW1222 cells. Figure 7 displays the viability curves obtained after incubation with A33-positive cells for 72 h. The IC<sub>50</sub> value was 0.5 μM for IMTXA33αS and 3.5 μM for scFvA33T1. When protein biosynthesis inhibition was analyzed in the same conditions the IC<sub>50</sub> values obtained were 30 nM and > 5 μM, respectively.

To assess the relationship between the cytotoxic efficiency and the intracellular pathway followed by the immunoconjugates IMTXA33αS or scFvA33T1, new *in vitro* cytotoxicity assays were performed including bafilomycin or brefeldin A as inhibitors of the lysosomal and Golgi functions, respectively [50,51]. As expected, scFvA33T1 toxicity was dramatically increased when bafilomycin was added, due to

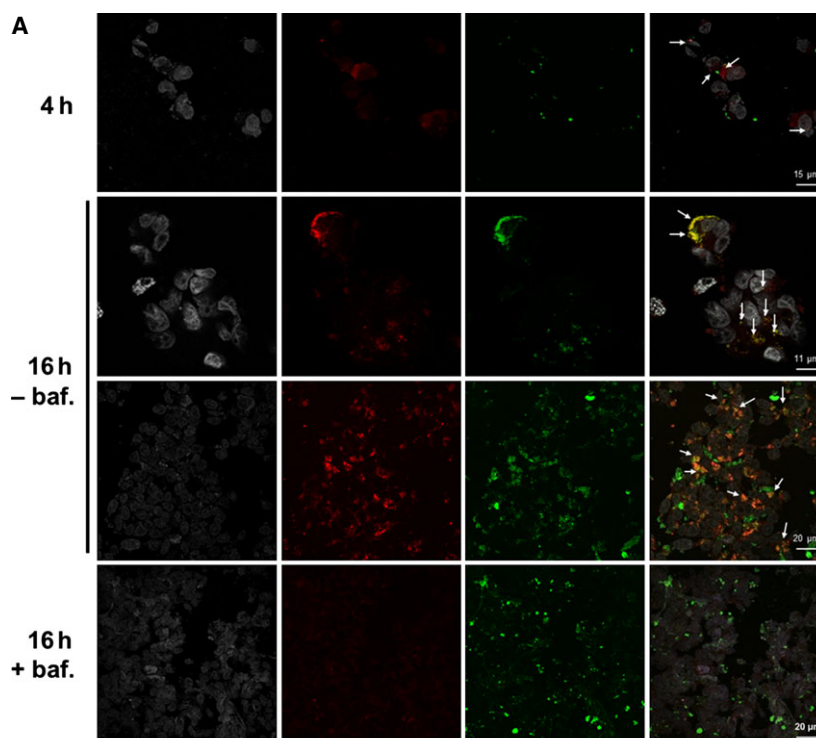


**Fig. 4.** Immunofluorescence confocal microscopy images of SW1222 cells incubated for 4 and 16 h with scFvA33T1-555 in the absence or presence of bafilomycin at  $5 \text{ ng}\cdot\text{mL}^{-1}$  to analyze colocalization with lysosomes. (A) Images correspond to (columns from left to right) nuclei labeled with DAPI, lysosomes labeled with Lysotracker, scFvA33T1-555 and merging of the three channels. Arrows indicate some sites of colocalization observed. (B) Quantitative colocalization analysis as indicated in Materials and methods.

Lysosomes colocalization	scFvA33T1 (4 h)	scFvA33T1 (16 h)	scFvA33T1 (16 h + bafilomycin)
Pearson's coefficient ( <i>r</i> )	0.093	0.687/0.425	0.012
Overlap coefficient (%)	26.9	49.2/58.1	1.3

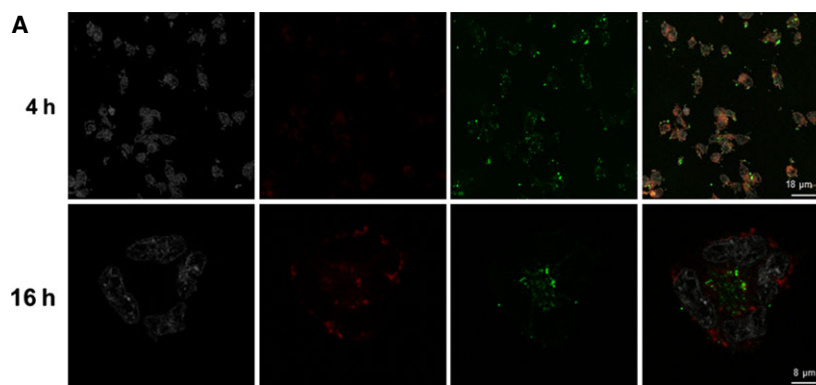


**Fig. 5.** Immunofluorescence confocal microscopy images of SW1222 cells incubated for 4 and 16 h with IMTXA33 $\alpha$ S-555 to analyze colocalization with lysosomes. (A) Images correspond to (columns from left to right) nuclei labeled with DAPI, lysosomes labeled with Lysotracker, IMTXA33 $\alpha$ S-555 and merging of the three channels. (B) Quantitative colocalization analysis as indicated in Materials and methods.

Lysosomes colocalization	IMTXA33 $\alpha$ S (4 h)	IMTXA33 $\alpha$ S (16 h)
Pearson's coefficient ( <i>r</i> )	0.05	0.11
Overlap coefficient (%)	3.8	4.7

inhibition of recycling in the lysosomes, with an  $\text{IC}_{50}$  value of  $70 \text{ nM}$  (Fig. 8), while no effect was observed when brefeldin A was added. On the other hand, IMTXA33 $\alpha$ S showed a significantly diminished toxicity

when brefeldin A was added, with an increase in the  $\text{IC}_{50}$  value up to  $0.5 \mu\text{M}$ . However, no effect was observed in this case after the addition of bafilomycin (Fig. 8).



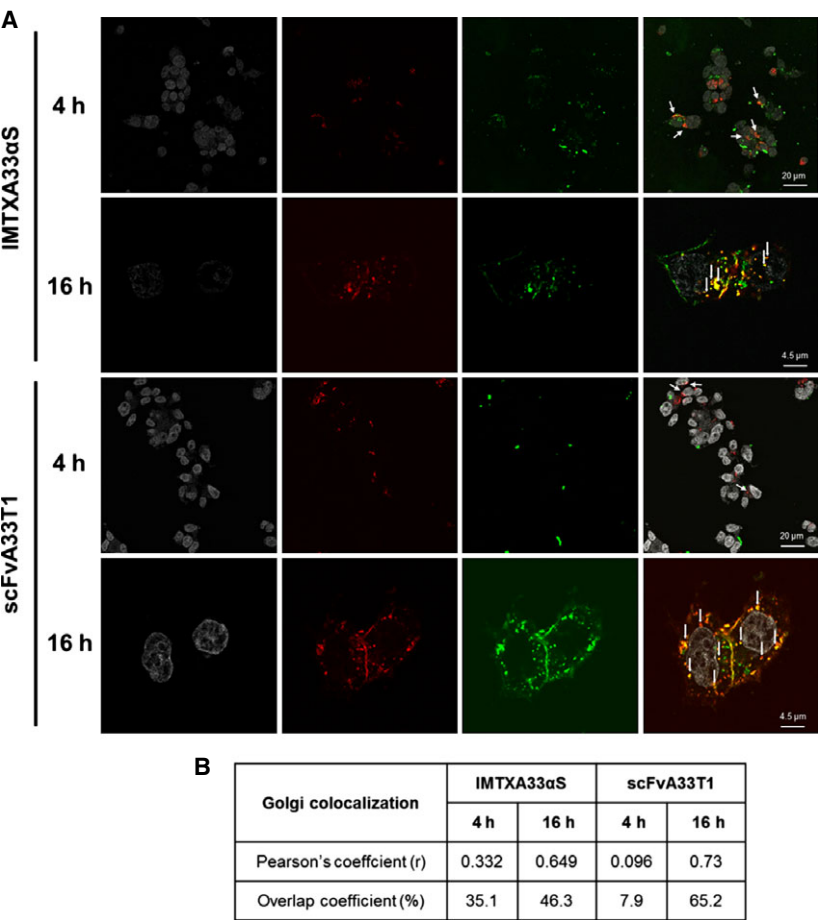


**Fig. 6.** Immunofluorescence confocal microscopy images of SW1222 cells incubated for 4 and 16 h with IMTXA33αS-555 or scFvA33T1-555 to analyze colocalization with the Golgi apparatus. (A) Images correspond to (columns from left to right) nuclei labeled with DAPI, Golgi labeled with agglutinin, IMTXA33αS-555 or scFvA33T1-555 and merging of the three channels. Arrows indicate some sites of colocalization. (B) Quantitative colocalization analysis as indicated in Materials and methods.

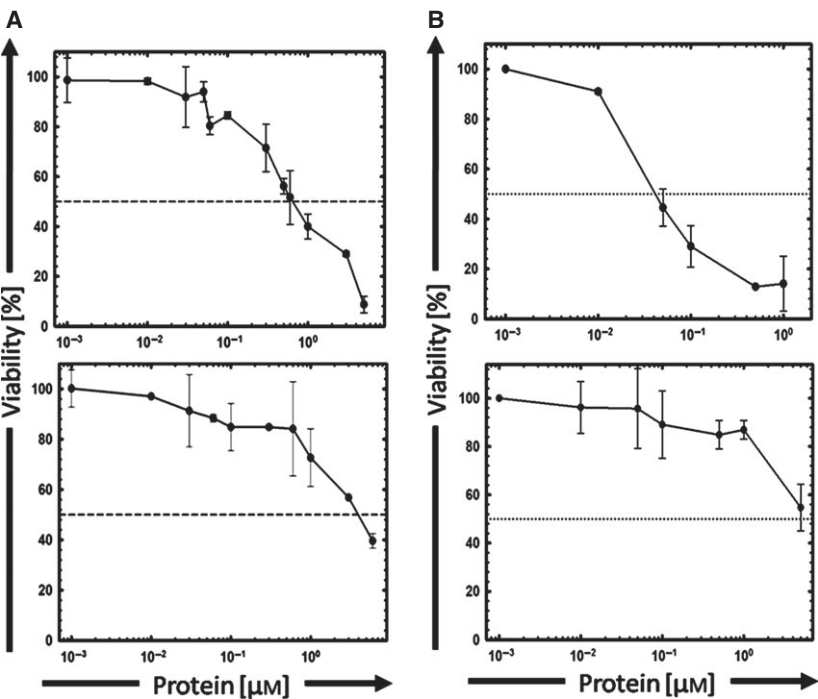


**Fig. 7.** Viability assay of SW1222 cells incubated for 72 h with IMTXA33αS (upper panel) or scFvA33T1 (bottom panel). The graphs on the left (A) correspond to the MTT assays, while the ones on the right (B) are protein biosynthesis inhibition experiments. The dotted line corresponds to the  $\text{IC}_{50}$  values, being  $0.5 \mu\text{M}$  for IMTXA33αS and  $3.5 \mu\text{M}$  for scFvA33T1 (MTT assays). The protein biosynthesis experiments yielded  $\text{IC}_{50}$  values of  $0.03 \mu\text{M}$  for IMTXA33αS and  $\sim 10 \mu\text{M}$  for scFvA33T1.

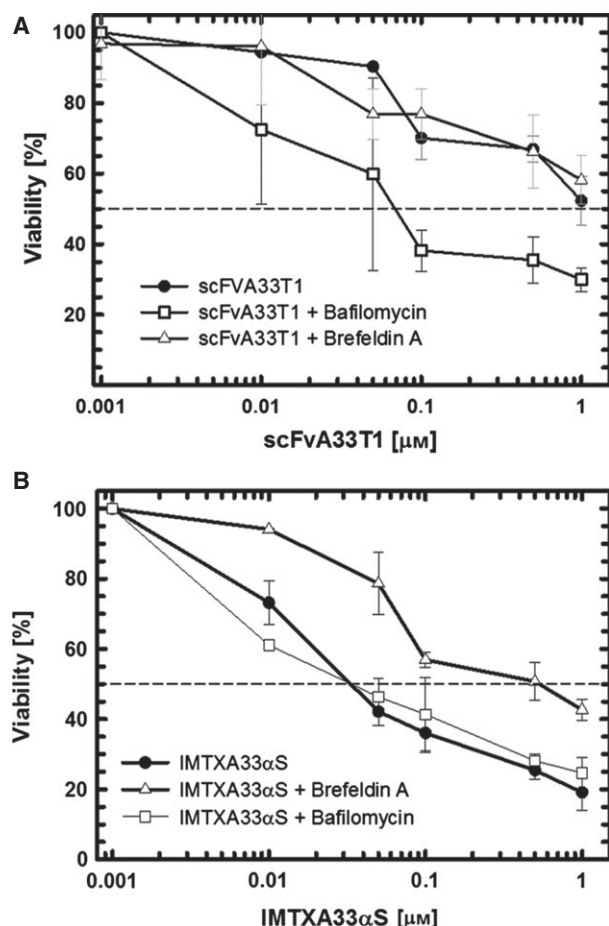


**Fig. 8.** Viability assay of SW1222 cells incubated for 72 h with scFvA33T1 (A) or IMTXA33 $\alpha$ S (B) and brefeldin A or bafilomycin. (A) MTT viability assay of SW1222 cells incubated with scFvA33T1 (●), scFvA33T1 + bafilomycin (□) and scFvA33T1 + brefeldin A (Δ), with  $\text{IC}_{50}$  values of 70 nM for scFvA33T1 + bafilomycin and  $> 1 \mu\text{M}$  for scFvA33T1 alone or with brefeldin A. (B) Protein biosynthesis inhibition assay of SW1222 cells incubated with IMTXA33 $\alpha$ S (●), IMTXA33 $\alpha$ S + bafilomycin (□) and IMTXA33 $\alpha$ S + brefeldin A (Δ), with  $\text{IC}_{50}$  values of 20–30 nM for IMTXA33 $\alpha$ S alone or with bafilomycin and 0.5  $\mu\text{M}$  for IMTXA33 $\alpha$ S with brefeldin A. The dashed line indicates the 50% level of protein biosynthesis inhibition used to calculate the  $\text{IC}_{50}$  values.

## Discussion

Over the last few years, evidence has accumulated to describe how the efficiency of immunotoxins depends on a large number of conditions [23,52,53]. These include the nature and reaction mechanism of the toxic domain [29,54,55], the type of tumor [28,56,57], the specificity and mechanism of binding [58,59] and the innate toxicity of the construct once the immunoconjugate reaches the tumor [53,60]. Within this idea, understanding the toxin intracellular pathway is crucial for improving the immunotoxin efficiency [4,20].

Consequently, in this report we have studied two immunoconjugates with the same binding domain but two different toxic moieties. Both showed identical specific binding to GPA33-positive cells, as described previously using flow cytometry and confocal microscopy [13,44]. Now it is shown how both immunoconjugates enter via early endosomes, one of the most common means of internalization [61]. This transit is indeed brief, as shown by the quick disappearance of the corresponding fluorescence signal related to endosome colocalization. However, these similarities disappear when the intracellular pathway followed by the toxic domain is analyzed (Fig. 9). Thus, the  $\alpha$ -sarcin based immunotoxin displays a clear preference for the endosome–Golgi apparatus pathway and translocates into the cytosol directly either from the endosomes or the Golgi apparatus, most probably as a result of the ability of  $\alpha$ -sarcin to interact with negatively charged membranes [62,63]. Interestingly, the construction containing RNase T1 was found both in the lysosomes and in the Golgi apparatus. In this case, the incapacity of RNase T1 to interact with membranes would hinder its release to the cytosol from the Golgi, as can be inferred by the increase in the colocalization fluorescence signal. Furthermore, the use of the lysosomal route would involve the proteolytic degradation of the immunoRNase, decreasing its cytotoxic efficacy.

These interpretations are further supported by the results obtained regarding the cytotoxic efficiency in the presence of brefeldin A or bafilomycin. Thus, when the vesicle transport through the Golgi apparatus is impaired due to the addition of brefeldin A, the cytotoxicity efficiency of IMTXA33 $\alpha$ S is diminished. However, when lysosomal recycling is the function disrupted, by bafilomycin, a significantly increased cytotoxicity was observed in the case of scFvA33T1.

Initially, the differences observed between both immunoconjugates in terms of antitumoral activity were explained by the exquisite specificity of  $\alpha$ -sarcin against ribosomes [13,42] in contrast with the much less specific action of RNase T1 [43,44]. That is, *a priori* many fewer  $\alpha$ -sarcin molecules would be needed to induce cell death. In fact, it has been estimated that just one molecule of this ribotoxin would be enough to efficiently kill one cell [64]. However, the results presented now suggest a more complex scenario where the intracellular pathway followed by each toxic moiety would also strongly influence the lethality of each immunoconjugate. The differences observed in their intracellular trafficking pathways are in fact in good agreement with the results of their cytotoxic action since IMTXA33 $\alpha$ S was found to be 7-fold higher. In this sense, both endosomes and Golgi apparatus inner

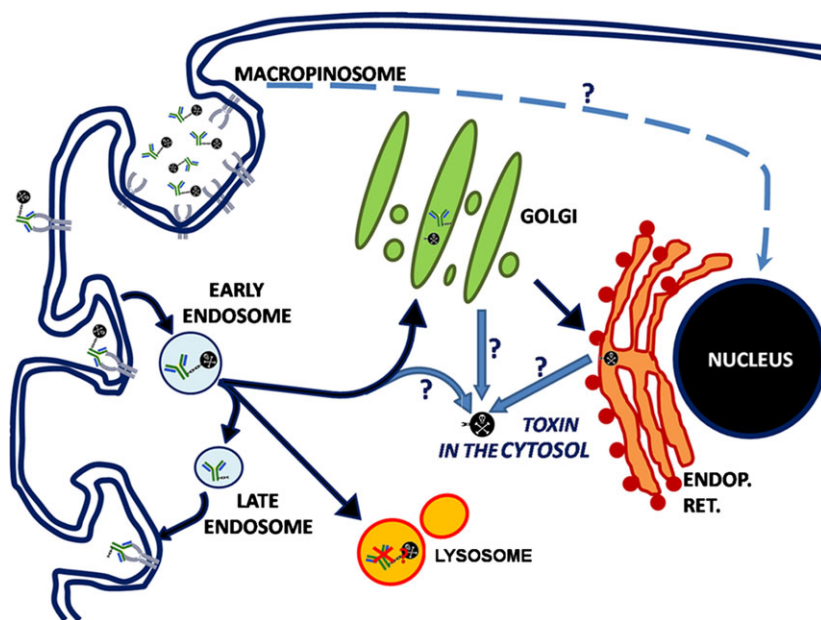


**Fig. 9.** Scheme representing the different intracellular pathways that can be followed by an immunoconjugate to release its toxic cargo into the cytosol.

membranes are rich in negative charges [65–68]. This negative charge environment most probably contributes to  $\alpha$ -sarcin translocation since it is well known that this protein takes advantage of the presence of negative acidic phospholipids to enter its target cells [42,62]. Thus,  $\alpha$ -sarcin delivery to the cytosol could be achieved directly from endosomes or from the Golgi apparatus. However, RNase T1, a protein with an acidic pI value [43,49], would not be able to interact with the endosome or Golgi membranes, resulting in an impairment of its release into the cytosol, favoring also recycling and degradation in the lysosomes or driving to the late Golgi.

In summary, the data reported here elucidate the different pathways followed by two thoroughly studied RNases when integrated into an antitumoral immunoconjugate and how their innate features affect the toxic behavior of the two immunotoxins assayed. Therefore,  $\alpha$ -sarcin based immunotoxins exhibit greater antitumoral activity than those based on RNase T1 not only because of the higher intrinsic lethal activity of  $\alpha$ -sarcin against ribosomes but also because it uses the Golgi intracellular pathway to reach the cytosol in a much more efficient way.

## Materials and methods

### Cell line culture

Colon carcinoma SW1222 cells were used as a standardized GPA33-positive cellular line [13,44]. This cell line was grown as described previously [44] in Dulbecco's modified

Eagle's medium containing glutamine ( $300 \text{ mg} \cdot \text{mL}^{-1}$ ),  $50 \text{ U} \cdot \text{mL}^{-1}$  of penicillin and  $50 \text{ mg} \cdot \text{mL}^{-1}$  of streptomycin. This medium was supplemented with 10% fetal bovine serum. Incubation was performed at  $37^\circ\text{C}$  in a humidified atmosphere ( $\text{CO}_2$  : air, 1 : 9 v/v). Harvesting and propagation of cultures were routinely performed by trypsinization. The number of cells used was determined in all assays by using a hemocytometer.

### Alexa 555 labeling of IMTXA33 $\alpha$ S and scFvA33T1

The absence of primary amine groups in the complementary determinant regions of the scFvA33 was previously checked to prevent modifications that could result in defective binding [69]. Then, the Alexa Fluor 555 Protein Labeling Kit (Invitrogen, Carlsbad, CA, USA) was used to label the proteins by incubating 2.6 nmol of IMTXA33 $\alpha$ S or scFvA33T1 with 44.6 nmol of Alexa 555 for 15 min at room temperature. The buffer used was 0.1 M sodium bicarbonate, pH 7.5 for the immunotoxin and pH 8.0 for the immunoRNase. Both Alexa 555 conjugates (IMTXA33 $\alpha$ S-555 and scFvA33T1-555) were purified using the resin provided with the kit. Finally, the degree of labeling was calculated according to the kit instructions.

### Far-UV circular dichroism

Far-UV CD spectra were obtained on a Jasco 715 spectropolarimeter at  $50 \text{ nm} \cdot \text{min}^{-1}$  scanning speed as described before [70]. Proteins were used at  $0.15 \text{ mg} \cdot \text{mL}^{-1}$  in PBS. Cells of 0.1 cm optical path were employed. At least four spectra were averaged to obtain the final data.



## Fluorescence microscopy

SW1222 cells were trypsinized, seeded at  $8 \times 10^5$  cells-well<sup>-1</sup> over cover-glasses placed into a 24-well plate, and incubated at 37 °C overnight. Cells were then treated with IMTXA33 $\alpha$ S-555 or scFvA33T1-555, at 25  $\mu$ g-mL<sup>-1</sup>, for different periods of time: 2 h for endosome colocalization, 4 or 16 h for lysosomes/Golgi and 16 h for overall internalization assays. To confirm colocalization of scFvA33T1 with lysosomes, bafilomycin at 5 ng-mL<sup>-1</sup> was added together with the immunoRNase, when necessary. To visualize the plasmatic membrane, cells were incubated with anti-CD44 mAb [71]. Then, medium was removed and cells were fixed for 15 min with PBS containing 3% (v/v) *p*-formaldehyde, followed by a 15-min incubation in PBS containing 50 mM ammonium chloride. Cells were permeabilized with digitonin at 0.01% (w/v) in PBS for 30 min, followed by PBS containing 1.0% (w/v) BSA for 1 h. For organelle labeling different probes were used: early endosomes were labeled with anti-EEA1 (Abcam, Cambridge, UK), lysosomes with LysoTracker (Life Technologies, Madrid, Spain) and Golgi apparatus with wheat germ agglutinin (Life Technologies), following the provider's instructions. DAM-Alexa 647 and goat anti-rabbit (GAR)-Alexa 488 were used as secondary antibodies. Finally, nuclei were labeled with 10  $\mu$ L of Prolong Gold with 4,6-diamidino-2-phenylindole (DAPI) (Life Technologies). All incubations were performed at room temperature and the final preparations were kept at 4 °C until further use. A Leica TCS SP2 confocal microscope and LCS LITE software were used to obtain the images. Starting at the basal zone of the cells and ending at the apical, 10 different images were taken along the *z*-axis for each preparation. Images correspond to slices 4–6, i.e. the optical planes corresponding to the internal content of the analyzed cells. For quantitative colocalization analysis, IMAGEJ software was used to calculate the Pearson correlation coefficient and the overlap coefficient according to Mander, which refer to the correlation of the intensity distribution between channels and true degree of colocalization, respectively [72].

## MTT viability assay

Cell viability was evaluated by MTT using the Cell Proliferation Kit I (Roche, Basel, Switzerland). This assay is based on the cleavage of the yellow tetrazolium salt MTT to purple formazan crystals by metabolic active cells. Trypsinized  $5 \times 10^3$  cells-well<sup>-1</sup> were seeded into a 96-well plate and incubated for 24 h at 37 °C in a humidified atmosphere. Then, the medium was removed and replaced with a new one containing IMTXA33 $\alpha$ S or scFvA33T1 at different concentrations in 200  $\mu$ L final volume. After an incubation time of 24 h, cells were further incubated with MTT at 0.5 mg-mL<sup>-1</sup> for 2 h at 37 °C, following the MTT kit instructions. Once this incubation was finished, the solubilization buffer was added and viability was measured in

terms of absorbance at 550 nm. A higher amount of viable cells corresponds to higher  $A_{550}$  values. Thus, readings obtained for cells incubated only with medium, in the absence of either IMTXA33 $\alpha$ S or scFvA33T1, were taken as 100% viability. When required, brefeldin A or bafilomycin at 1 or 5 ng-mL<sup>-1</sup> respectively were added together with the immunoconjugates. Controls with brefeldin A or bafilomycin without the immunoconjugates were performed to consider drug related toxicity. Results shown are the average of four independent assays.

## Protein biosynthesis inhibition

Ribotoxins exert their cellular cytotoxicity by inactivating ribosomes, leading to protein biosynthesis inhibition and cellular death [42]. Thus, protein biosynthesis is the activity routinely used to evaluate the toxic effect of this family of proteins [49,63]. Consequently, to evaluate the effect of IMTXA33 $\alpha$ S or scFvA33T1, cells were seeded into 96-well plates at  $1 \times 10^4$  cells-well<sup>-1</sup> in culture medium and maintained under standard culture conditions for 36 h. Then the monolayer cultures were incubated with 0.2 mL of fresh medium in the presence of different concentrations of IMTXA33 $\alpha$ S or scFvA33T1. Following 72 h of incubation at 37 °C, the medium was removed and replaced with fresh medium supplemented with 1  $\mu$ Ci-well<sup>-1</sup> of L-[4,5-<sup>3</sup>H]-leucine (166 Ci-mmol<sup>-1</sup>; GE Healthcare UK Ltd, Buckinghamshire, UK). After an additional incubation of 6 h, this medium was also removed; cells were fixed with 5.0% (w/v) trichloroacetic acid and washed three times with cold ethanol. The resulting dried pellet was dissolved in 0.2 mL of 0.1 M NaOH containing 0.1% SDS, and its radioactivity was counted on a Beckman LS3801 liquid scintillation counter. The results were expressed as percentage of the radioactivity incorporated in control samples incubated without either of the two immunoconjugates to calculate IC<sub>50</sub> values (protein concentration inhibiting 50% protein synthesis) in the cytotoxicity assays. When required, brefeldin A or bafilomycin at 1 or 5 ng-mL<sup>-1</sup> respectively was added together with the immunoconjugates. Controls with brefeldin A or bafilomycin without the immunoconjugates were performed to consider drug related toxicity. Three independent replicate assays were conducted to calculate the average IC<sub>50</sub> values.

## Acknowledgements

This work was supported by grant BFU2012-32404 from the Spanish Ministerio de Economía y Competitividad.

## Author contributions

JT-A planned and performed experiments, analyzed data and wrote the paper. JR-H planned and per-

formed experiments and analyzed data. AM-P analyzed data and revised the paper. JGG analyzed data and revised the paper. JL planned experiments, analyzed data and wrote the paper.

## References

- Gensini GF, Conti AA & Lippi D (2007) The contributions of Paul Ehrlich to infectious disease. *J Infect* **54**, 221–224.
- Holzman DC (2009) Whatever happened to immunotoxins? Research and hope, are still alive *J Natl Cancer Inst* **101**, 624–625.
- Madhumathi J & Verma RS (2012) Therapeutic targets and recent advances in protein immunotoxins. *Curr Opin Microbiol* **15**, 300–309.
- Frankel AE, Woo JH & Neville DM (2009) Immunotoxins. In *Principles of Cancer Biotherapy* (Oldham RK & Dillman RO, eds), pp. 407–449. Springer, Netherlands.
- Nielsen K & Boston RS (2001) Ribosome-inactivating proteins: A Plant Perspective. *Annu Rev Plant Physiol* **52**, 785–816.
- Muñoz R, Arias Y, Ferreras JM, Jiménez P, Rojo MA & Gírbés T (2001) Sensitivity of cancer cell lines to the novel non-toxic type 2 ribosome-inactivating protein nigrin b. *Cancer Lett* **167**, 163–169.
- Pirie CM, Hackel BJ, Rosenblum MG & Wittrup KD (2011) Convergent potency of internalized gelonin immunotoxins across varied cell lines, antigens, and targeting moieties. *J Biol Chem* **286**, 4165–4172.
- Günhan E, Swe M, Palazoglu M, Voss JC & Chalupa LM (2008) Expression and purification of cysteine introduced recombinant saporin. *Protein Expr Purif* **58**, 203–209.
- Wang Z, Duran-Struuck R, Crepeau R, Matar A, Hanekamp I, Srinivasan S, Neville DM Jr, Sachs DH & Huang CA (2011) Development of a diphtheria toxin based antiporcine CD3 recombinant immunotoxin. *Bioconjug Chem* **22**, 2014–2020.
- Liu XF, FitzGerald DJ & Pastan I (2013) The insulin receptor negatively regulates the action of *Pseudomonas* toxin-based immunotoxins and native *Pseudomonas* toxin. *Cancer Res* **73**, 2281–2288.
- Frankel AE, Powell BL, Hall PD, Case LD & Kreitman RJ (2002) Phase I trial of a novel diphtheria toxin/granulocyte macrophage colony-stimulating factor fusion protein (DT388GMCSF) for refractory or relapsed acute myeloid leukemia. *Clin Cancer Res* **8**, 1004–1013.
- Edelweiss E, Balandin TG, Stremovskiy OA, Deyev SM & Petrov RV (2010) Anti-EGFR-Miniantibody-Barnase immunoconjugate is highly toxic for human tumor cells. *Dokl Akad Nauk SSSR* **434**, 558–561.
- Carreras-Sangrà N, Tomé-Amat J, García-Ortega L, Batt CA, Oñaderra M, Martínez-del-Pozo A, Gavilanes JG & Lacadena J (2012) Production and characterization of a colon cancer-specific immunotoxin based on the fungal ribotoxin  $\alpha$ -sarcin. *Protein Eng Des Sel* **25**, 425–435.
- Zhou H, Marks JW, Hittelman WN, Yagita H, Cheung LH, Rosenblum MG & Winkles JA (2011) Development and characterization of a potent immunoconjugate targeting the Fn14 receptor on solid tumor cells. *Mol Cancer Ther* **10**, 1276–1288.
- Bremer E, de Bruyn M, Wajant H & Helfrich W (2009) Targeted cancer immunotherapy using ligands of the tumor necrosis factor superfamily. *Curr Drug Targets* **10**, 94–103.
- Avila AD, Mateo de Acosta C & Lage A (1988) A new immunotoxin built by linking a hemolytic toxin to a monoclonal antibody specific for immature T lymphocytes. *Int J Cancer* **42**, 568–571.
- García-Ortega L, Alegre-Cebollada J, García-Linares S, Bruix M, Martínez-Del-Pozo A & Gavilanes JG (2011) The behavior of sea anemone actinoporins at the water-membrane interface. *Biochim Biophys Acta* **1808**, 2275–2288.
- Al-yahyaee SAS & Ellar DJ (1996) Cell targeting of a pore-forming toxin, CytA  $\delta$ -Endotoxin from *Bacillus thuringiensis* subspecies israelensis, by conjugating CytA with anti-thy 1 monoclonal antibodies and insulin. *Bioconjug Chem* **7**, 451–460.
- Hexham JM, Dudas D, Hugo R, Thompson J, King V, Dowling C, Neville DM Jr, Digan ME & Lake P (2001) Influence of relative binding affinity on efficacy in a panel of anti-CD3 scFv immunotoxins. *Mol Immunol* **38**, 397–408.
- Johannes L & Decaudin D (2005) Protein toxins: intracellular trafficking for targeted therapy. *Gene Ther* **12**, 1360–1368.
- Chames P, Regenmortel MV, Weiss E & Baty D (2009) Therapeutic antibodies: successes, limitations and hopes for future. *Br J Pharmacol* **159**, 220–223.
- Cao Y, Mohamedali KA, Marks JW, Cheung LH, Hittelman WN & Rosenblum MG (2013) Construction and characterization of novel, completely human serine protease therapeutics targeting Her2/neu. *Mol Cancer Ther* **12**, 979–991.
- Becker N & Benhar I (2012) Antibody-based immunotoxins for the treatment of cancer. *Antibodies* **1**, 39–69.
- Woo BH, Lee JT, Park MO, Lee KR, Han JW, Park ES, Yoo SD & Lee KC (1999) Stability and cytotoxicity of Fab-ricin A immunotoxins prepared

- with water soluble long chain heterobifunctional crosslinking agents. *Arch Pharm Res* **22**, 459–463.
- 25 Qiu XQ, Wang H, Cai B, Wang LL & Yue ST (2007) Small antibody mimetics comprising two complementarity-determining regions and a framework region for tumor targeting. *Nat Biotechnol* **25**, 92–929.
  - 26 Liu W, Onda M, Kim C, Xiang L, Weldon JE, Lee B & Pastan I (2012) A recombinant immunotoxin engineered for increased stability by adding a disulfide bond has decreased immunogenicity. *Protein Eng Des Sel* **25**, 1–6.
  - 27 Rybak SM (2008) Antibody-onconase conjugates: cytotoxicity and intracellular routing. *Curr Pharm Biotechnol* **9**, 226–230.
  - 28 Zhang Y, Xiang L, Hassan R & Pastan I (2007) Immunotoxin and Taxol synergy results from a decrease in shed mesothelin levels in the extracellular space of tumors. *Proc Natl Acad Sci USA* **104**, 17099–17104.
  - 29 Mossoba ME, Onda M, Taylor J, Massey PR, Treadwell S, Sharon E, Hassan R, Pastan I & Fowler DH (2011) Pentostatin plus cyclophosphamide safely and effectively prevents immunotoxin immunogenicity in murine hosts. *Clin Cancer Res* **17**, 3697–3705.
  - 30 Todorovska A, Roovers RC, Dolezal O, Kortt AA, Hoogenboom HR & Hudson PJ (2001) Design and application of diabodies, triabodies and tetrabodies for cancer targeting. *J Immunol Methods* **248**, 47–66.
  - 31 Kim KM, McDonagh CF, Westendorf L, Brown LL, Sussman D, Feist T, Lyon R, Alley SC, Okeley NM, Zhang X *et al.* (2008) Anti-CD30 diabody-drug conjugates with potent antitumor activity. *Mol Cancer Ther* **7**, 2486–2497.
  - 32 Asano R, Ikoma K, Shimomura I, Taki S, Nakanishi T, Umetsu M & Kumagai I (2011) Cytotoxic enhancement of a bispecific diabody by format conversion to tandem single-chain variable fragment (taFv): the case of the hEx3 diabody. *J Biol Chem* **286**, 812–818.
  - 33 De Lorenzo C & D'Alessio G (2008) From immunotoxins to immunoRNases. *Curr Pharm Biotechnol* **9**, 210–214.
  - 34 Balandin TG, Edelweiss E, Andronova NV, Treshalina EM, Sapozhnikov AM & Deyev SM (2011) Antitumor activity and toxicity of anti-HER2 immunoRNase scFv 4D5-dibarnase in mice bearing human breast cancer xenografts. *Invest New Drugs* **29**, 22–32.
  - 35 Borriello M, Lacceti P, Terrazzano G, D'Alessio G & De Lorenzo C (2011) A novel fully human antitumor immunoRNase targeting ErbB2-positive tumors. *Br J Cancer* **104**, 1716–1723.
  - 36 Deckert PM, Renner C, Cohen LS, Jungnluth A, Ritter G, Bertino JR, Old LJ & Welt S (2003) A33scFv-cytosine deaminase: a recombinant protein construct for antibody-directed enzyme-prodrug therapy. *Br J Cancer* **88**, 937–939.
  - 37 Weldon JE & Pastan I (2011) A guide to taming a toxin-recombinant immunotoxins constructed from *Pseudomonas* exotoxin A for the treatment of cancer. *FEBS J* **278**, 4683–4700.
  - 38 Weng A, Thakur M, von Mallinckradt B, Beceren-Braun F, Gilabert-Oriol R, Wiesner B, Eickhart J, Böttger S, Melzig MF & Fuchs H (2012) Saponins modulate the intracellular trafficking of protein toxins. *J Control Release* **164**, 74–86.
  - 39 Ritter G, Cohen LS, Nice EC, Catimel B, Burgess AW, Moritz RL, Ji H, Heath JK, White SJ, Welt S *et al.* (1997) Characterization of posttranslational modifications of human A33 antigen, a novel palmitoylated surface glycoprotein of human gastrointestinal epithelium. *Biochem Biophys Res Commun* **236**, 682–686.
  - 40 Pereira-Fantini PM, Judd LM, Kalantzis A, Peterson A, Ernst M, Heath JK & Giraud AS (2010) A33 antigen-deficient mice have defective colonic mucosal repair. *Inflamm Bowel Dis* **16**, 604–612.
  - 41 Daghighian F, Barendswaard E, Welt S, Humm J, Scott A, Willingham MC, McGuffie E, Old LJ & Larson SM (2007) Enhancement of radiation dose to the nucleus by vesicular internalization of iodine-125-labeled A33 monoclonal antibody. *J Nucl Med* **37**, 1052–1057.
  - 42 Lacadena J, Alvarez-García E, Carreras-Sangrà N, Herrero-Galán E, Alegre-Cebollada J, García-Ortega L, Oñaderra M, Gavilanes JG & Martínez-del-Pozo A (2007) Fungal ribotoxins: molecular dissection of a family of natural killers. *FEMS Microbiol Rev* **31**, 212–237.
  - 43 Yoshida H (2001) The ribonuclease T1 family. *Methods Enzymol* **341**, 28–41.
  - 44 Tomé-Amat J, Menéndez-Méndez A, García-Ortega L, Batt CA, Oñaderra M, Martínez-del-Pozo A, Gavilanes JG & Lacadena J (2012) Production and characterization of scFvA33T1, an immunoRNase targeting colon cancer cells. *FEBS J* **279**, 3022–3032.
  - 45 Martínez-del-Pozo A, Gasset M, Oñaderra M & Gavilanes JG (1988) Conformational study of the antitumor protein  $\alpha$ -sarcin. *Biochim Biophys Acta* **953**, 280–288.
  - 46 Nazarewicz RR, Salazar G, Patrushev N, San Martin A, Hilenski L, Xiong S & Alexander RW (2011) Early endosomal antigen 1 (EEA1) is an obligate scaffold for angiotensin II-induced, PKC- $\alpha$ -dependent Akt activation in endosomes. *J Biol Chem* **286**, 2886–2895.
  - 47 Anderson RG & Orci L (1988) A view of acidic intracellular compartments. *J Cell Biol* **106**, 539–543.
  - 48 Zhao W, Chen TL, Vertel BM & Colley KJ (2006) The CMP-sialic acid transporter is localized in the medial-trans Golgi and possesses two specific endoplasmic

- reticulum export motifs in its carboxyl-terminal cytoplasmic tail. *J Biol Chem* **281**, 31106–31118.
- 49 Martínez-Ruiz A, García-Ortega L, Kao R, Lacadena J, Oñaderra M, Mancheño JM, Davies J, Martínez del Pozo A & Gavilanes JG (2001) RNase U2 and  $\alpha$ -sarcin: a study of relationships. *Meth Enzymol* **341**, 335–351.
  - 50 Yoshimori T, Yamamoto A, Moriyama Y, Futai M & Tashiro Y (1991) Bafilomycin A<sub>1</sub>, a specific inhibitor of vacuolar-type H<sup>+</sup>-ATPase, inhibits acidification and protein degradation in lysosomes of cultured cell. *J Biol Chem* **266**, 17707–17712.
  - 51 Fujiwara T, Oda K, Yokota S, Takatsuki A & Ikehara Y (1988) Brefeldin A causes disassembly of the Golgi complex and accumulation of secretory proteins in the endoplasmic reticulum. *J Biol Chem* **263**, 18545–18552.
  - 52 Dosio F, Brusa P & Cattel L (2011) Immunotoxins and anticancer drug conjugate assemblies: the role of the linkage between components. *Toxins* **3**, 848–883.
  - 53 Weldon JE, Xiang L, Zhang J, Beers R, Walker DA, Onda M, Hassan R & Pastan I (2013) A recombinant immunotoxin against the tumor-associated antigen mesothelin reengineered for high activity, low off-target toxicity, and reduced antigenicity. *Mol Cancer Ther* **12**, 48–57.
  - 54 Mellman I, Coukos G & Dranoff G (2011) Cancer immunotherapy comes of age. *Nature* **480**, 480–489.
  - 55 Topalian SL, Weiner GJ & Pardoll DM (2011) Cancer immunotherapy comes of age. *J Clin Oncol* **29**, 4828–4836.
  - 56 Messmer D & Kipps TJ (2005) Treatment of solid tumors with immunotoxins. *Breast Cancer Res* **7**, 184–186.
  - 57 Xiang X, Phung Y, Feng M, Nagashima K, Zhang J, Broadbudd VC, Hassan R, Fitzgerald D & Ho M (2011) The development and characterization of a human mesothelioma in vitro 3D model to investigate immunotoxin therapy. *PLoS ONE* **6**, e14640.
  - 58 Adams GP, Schier R, McCall AM, Simmons HH, Horak EM, Alpaugh RK, Marks JD & Weiner LM (2001) High affinity restricts the localization and tumor penetration of Single-Chain Fv antibody molecules. *Cancer Res* **61**, 4750–4755.
  - 59 Zhang F, Shan L, Liu Y, Neville D, Woo JH, Chen Y, Korotcov A, Lin S, Huang S, Sridhar R *et al.* (2013) An anti-PSMA bivalent immunotoxin exhibits specificity and efficacy for prostate cancer imaging and therapy. *Adv Healthc Mater* **2**, 736–744.
  - 60 Byers VS, Pawluczyk IZA, Hooi DSW, Price MR, Carroll S, Embleton MJ, Garnett MC, Berry N, Robins RA & Baldwin RW (1991) Endocytosis of immunotoxin-791T/36-RTA by tumor cells in relation to its cytotoxic action. *Cancer Res* **51**, 1990–1995.
  - 61 Le Roy C & Wrana JL (2005) Clathrin- and non-clathrin-mediated endocytic regulation of cell signalling. *Nat Rev Mol Cell Biol* **6**, 112–126.
  - 62 Gasset M, Martínez del Pozo A, Oñaderra M & Gavilanes JG (1989) Study of the interaction between the antitumor protein  $\alpha$ -sarcin and phospholipid vesicles. *Biochem J* **258**, 569–575.
  - 63 Olmo N, Turnay J, González de Buítrago G, López de Silanes I, Gavilanes JG & Lizarbe MA (2001) Cytotoxic mechanism of the ribotoxin  $\alpha$ -sarcin. Induction of cell death via apoptosis. *Eur J Biochem* **268**, 2113–2123.
  - 64 Lamy B, Davies J & Schindler D (1992) The *Aspergillus* ribonucleolytic toxins (ribotoxins). In *Genetically Engineered Toxins* (Frankel AE ed), pp. 237–258. Marcel Dekker, New York.
  - 65 Gruenberg J (2003) Lipids in endocytic membrane transport and sorting. *Curr Opin Cell Biol* **15**, 382–388.
  - 66 Bissing C & Gruenberg J (2013) Lipid sorting and multivesicular endosome biogenesis. *Cold Spring Harb Perspect Biol* **5**, a016816.
  - 67 Van Meer G, Voelker DR & Feigenson GW (2008) Membrane lipids: where they are and how they behave. *Nat Rev Mol Cell Biol* **9**, 112–124.
  - 68 Zhao P, Liu F, Zhang B, Liu X, Wang B, Gong J, Yu G, Ma M, Lu Y, Sun J *et al.* (2013) MAIGO2 is involved in abscisic acid-mediated response to abiotic stresses and Golgi-to-ER retrograde transport. *Physiol Plant* **148**, 246–260.
  - 69 King DJ, Antoniw P, Owens RJ, Adair JR, Haines AM, Farnsworth AP, Finney H, Lawson AD, Lyons A & Baker TS (1995) Preparation and preclinical evaluation of humanised A33 immunoconjugates for radioimmunotherapy. *Br J Cancer* **72**, 1364–1372.
  - 70 Lacadena J, Martínez-del-Pozo A, Martínez A, Pérez JM, Bruix M, Mancheño JM, Oñaderra M & Gavilanes JG (1999) Role of His-50, Glu-96 and His-137 in the ribonucleolytic mechanism of ribotoxin  $\alpha$ -sarcin. *Proteins* **37**, 474–484.
  - 71 Yeung TM, Shaan CG, Wilding JL, Muschel R & Bodmer WF (2009) Cancer stem cells from colorectal cancer-derived cell lines. *Proc Natl Acad Sci USA* **107**, 3722–3727.
  - 72 Zinchuk V, Zinchuk O & Okada T (2007) Quantitative colocalization analysis of multicolor confocal immunofluorescence microscopy images: pushing pixels to explore biological phenomena. *Acta Histochem Cytochem* **40**, 101–111.